Formation of Molecular Iodine from the Two-Photon Dissociation of CI_4 and CHI_3: An Experimental and Computational Study

Eric D. Tweeten, Benjamin J. Petro, and Robert W. Quandt*

Department of Chemistry, Illinois State University, Normal, Illinois 61790-4160

Received: July 15, 2002; In Final Form: October 22, 2002

The formation of electronically excited molecular iodine from the two-photon photodissociation of CI_4 and CHI_3 was investigated using dispersed fluorescence and ab initio calculations. Molecular iodine was formed in the D, D′, and E ion-pair states from both CI_4 and CHI_3. In the photodissociation of CHI_3, the intensity of the D′ band is decreased and the E band is increased relative to those from CI_4. This intensity shift is explained in terms of the energetics of the carbene photofragments. Intrinsic reaction coordinate calculations were performed at the MP2 level of theory using the LANL2DZ basis set to characterize the dissociation pathways for CI_4 and CHI_3. The results of the calculations show the presence of three transition states and an ion-pair isomer intermediate for both molecules. The structure of the transition states for the formation of molecular iodine is in agreement with the asynchronous concerted dissociation mechanism proposed by Dantus and co-workers for CX_2Y_2 halocarbons.

I. Introduction

The photodissociation of halocarbons has received much interest due to the role these species play in stratospheric ozone depletion and as greenhouse gases.[1] The formation of atomic halogens, in both the $^2P_{1/2}$ and $^2P_{3/2}$ spin states, upon excitation to low-lying energy states of halocarbon parent molecules has been extensively studied.[2] However, in recent years, the formation of electronically excited *molecular* halogens from multiphoton dissociation of halocarbons has received renewed interest.

In a series of papers, Dantus and co-workers studied the femtosecond photodissociation dynamics of several *gem*-dihaloalkanes[3,4] and other mixed dihaloalkanes.[5] In their work, they found that with 96 154 $cm^{-1}$of excitation energy the molecular iodine photoproduct was formed primarily in the D′ ion-pair state. They also found that the dissociation was fast ($\tau < 50$ fs) and proceeded through an asynchronous concerted mechanism. Farmanara et al. found similar results in their studies of CF_2I_2.[6]

While several groups have looked at the photodissociation of CX_2Y_2 halocarbons, where X = H or F and Y = Cl, Br, or I, little or no work has been done on CXY_3 or CY_4 molecules. In this work, we report the formation of highly excited molecular iodine from the two-photon photodissociation of both CI_4 and CHI_3. The photodissociations were studied using both dispersed fluorescence and ab intio computational methods.

II. Experimental Section

The experimental technique used consists of flowing ∼50−250 mTorr of CI_4 (Aldrich Chemicals), CHI_3 (Eastman), or, for comparative purposes, neat I_2 (Mallinckrodt) through an 8 cm cubic cell made of stainless steel with five fused silica windows. The back window of the cell was offset by an additional 8 cm with an aluminum tube to reduce scatter. The 193 nm photolysis source was an ArF excimer laser (Lambda Physik, Compex 110) operating at 10 Hz and 100 mJ. The excimer beam was focused into the cell with a quartz lens ($f = 120$ mm) with great care being taken to ensure that the focal point was in the aluminum tube to prevent the absorption of three or more photons in the probe region. It should be noted that without the quartz lens no fluorescence was observed. With the quartz lens in place, intense fluorescence signals were seen for both CHI_3 and CI_4 and were attributed to photoproduct emission. This fluorescence was collected at right angles to the excimer beam with either a photomultiplier tube (Electron Tubes Limited model 9129b) for the time and power dependence studies or a collimating lens coupled to a fiber optic cable for the dispersed fluorescence work. The fiber optic then transmitted the collected light to an asymmetric crossed Czerny−Turner monochromator (Ocean Optics model S2000). An effective slit width of 8 mm and a 600 lines/mm grating give the monochromator a resolution of 1 nm. The dispersed light was detected with a CCD array, and the resulting signal was stored on a personal computer for later analysis. All chemicals, with the exception of CI_4, were used without further purification. The CI_4 was washed with a saturated sodium thiosulfate and water solution to remove any residual I_2. All chemicals were stored in opaque containers, and in a freezer when not in use, to minimize photodegradation.

III. Computational Section

The Gaussian 98[7] electronic structure package was utilized on either a Linux-based personal computer or a Silicon Graphics O2 workstation for all calculations. To account for relativistic effects, all of the calculations employed the LANL2DZ basis, which consists of the Los Alamos effective core potential plus double-ζ valence-only basis for iodine.[8−10] For first row atoms, the D95 double-ζ basis was used, leading to 41 basis functions for CI_4 (35 for CHI_3).[11] Geometries and transition-state structures were optimized at the MP2 level of theory. Convergence criteria for the geometry optimizations were that the rms gradient was less than or equal to 3×10^{-4} and the maximum component of the gradient was less than or equal to 1.2×10^{-3}. Single-point energies, at the MP4 level of theory using the same basis set, were then determined for the optimized structures. Neither the MP2 nor MP4 values were corrected for vibrational zero-point energies.

10.1021/jp021610j CCC: $25.00
Published on Web 11/27/2002

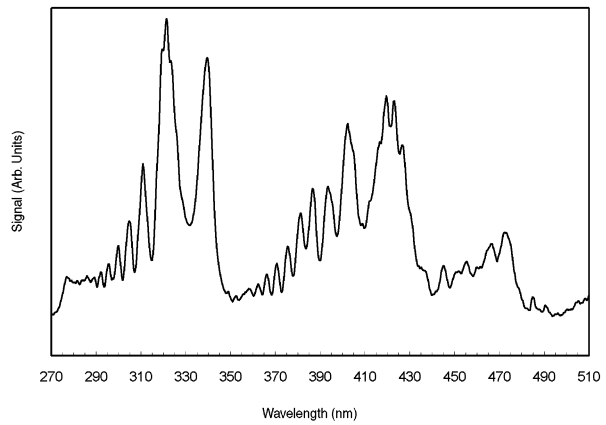

Figure 1. Dispersed photoproduct fluorescence spectra from the 2 × 193 nm photodissociation of CI_4. The data shown are an average of several spectra and were corrected by subtracting an averaged background signal that was obtained in the absence of CI_4.

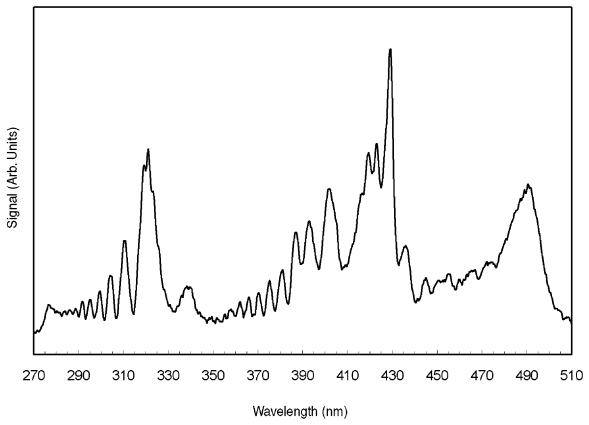

Figure 2. Dispersed photoproduct fluorescence spectra from the 2 × 193 nm photodissociation of CHI_3. The data shown are an average of several spectra and were corrected by subtracting an averaged background signal that was obtained in the absence of CHI_3.

All transition states were confirmed by the presence of a single imaginary frequency in the vibrational analysis, and intrinsic reaction coordinate (IRC) calculations were run at the MP2 level of theory to verify that they corresponded to the correct reactants and products. In addition, a natural bond orbital (NBO) analysis[12] was carried out for all reactants, products, and transition states, once again at the MP2 level of theory, to determine the charge distribution using natural population analysis.[13,14]

IV. Results and Discussion

A. Power Dependence. Upon excitation with focused 193 nm light, both CI_4 and CHI_3 exhibit strong UV and visible photoproduct fluorescence; however, upon removal of the focusing lens, this fluorescence disappears. To determine the number of photons involved in the photodissociation, the photoproduct fluorescence intensity as a function photolysis laser power was measured. A least-squares fit of the data gave power dependence values of 1.59 ± 0.17 for CI_4 and 1.80 ± 0.20 for CHI_3 indicating a two-photon process in each molecule. This is consistent with the results of Bersohn and co-workers for diiodomethane and iodoform.[15] They found that there is a barrier to the formation of molecular iodine from low-energy states ($<40\,000$ cm^{-1} for CH_2I_2 and $<35\,000$ cm^{-1} for CHI_3) because of symmetry constraints. Even at energies up to 82 237 cm^{-1}, molecular elimination is a minor channel.[16−18] It is only at energies greater than 96 000 cm^{-1} that the molecular channel becomes important. In this work, the two 193 nm photons have 103 627 cm^{-1} of energy, which is enough to form the molecular product for diiodomethane. Both CI_4 and CHI_3 would be expected to exhibit similar behavior albeit with lower barriers into the molecular elimination channel.

B. Dispersed Fluorescence. The dispersed fluorescence spectra obtained by focusing the 193 nm excimer laser into samples of CI_4 and CHI_3 are shown in Figures 1 and 2, respectively.

To confirm the identity of the fluorescing species, a two-photon spectrum for neat I_2, shown in Figure 3, was taken under the same conditions as those for CI_4 and CHI_3. A quick perusal of the figure and comparison to the one-photon spectra of Hemmati et al. clearly identifies the fluorescing species as molecular iodine.[19]

While I_2 is clearly the fluorescing species, it is, of course, possible that it may not be a photoproduct. The assignment of molecular iodine as a primary photoproduct was made for

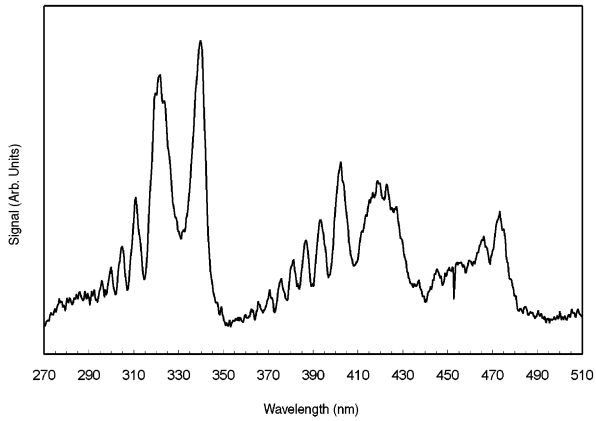

Figure 3. Dispersed laser-induced fluorescence (LIF) spectra from the 2 × 193 nm excitation of neat I_2. The data shown are an average of several spectra and were corrected by subtracting an averaged background signal that was obtained in the absence of I_2.

several reasons. First, while I_2 is a known contaminant of CI_4, the spectra showed virtually no change before and after purification with sodium thiosulfate, which is an effective scavenger of molecular halogens. Also, the spectra in all three figures were taken with equimolar amounts of CI_4, CHI_3, and I_2, yet the intensity of the fluorescence from the neat I_2 was ∼10 times weaker than that from the other two species. An opposite result would be expected if I_2 contaminant was the fluorescing species. Second, at the pressures used, typically around 100 mTorr, formation of molecular iodine from processes such as reactions 1−3 below would be expected to take several microseconds.

$$CI_4\ (\text{or } CHI_3) + h\nu\ (193\ \text{nm}) \rightarrow CI_3\ (CHI_2) + I \quad (1)$$

$$I + CI_4\ (CHI_3) \rightarrow CI_3\ (CHI_2) + I_2 \quad (2)$$

$$I + I + M \rightarrow I_2 + M \quad (3)$$

However, in all cases, the rise time of the fluorescence was detector-limited (<30 ns), precluding formation of I_2 from secondary reactions.

Several of the common features of the fluorescence spectra are of interest. The series of bands from 270 to 321 nm, as well as those from 355 to 402 nm, show evidence of Condon's internal diffraction effect indicating a transition from a bound upper state to a continuum lower state. The shorter wavelength

series is due to the well-known McLennan's diffuse band [D(1441, $^1\Sigma_u^+$) → X(2440, $^1\Sigma_g^+$)], while the upper band is likely due to transitions from the D state to the continuum of the 2422 $^3\Sigma_{g(O^+)}$ repulsive state or perhaps 2341 $^3\Sigma_{O^+g}$. Note that the numbering system of Mulliken is used. In this system, the digits stand for the number of electrons in the σ_g, π_u, π_g, and σ_u valence orbitals of I_2.[20]

Of greater interest are the bands centered at 340, 420, and 490 (CHI_3 only) nm. The first is the well-known D′(1432, $^3\Pi_{2g}$) → A′(2431, $^3\Pi_{2u}$) transition, the second is most likely the E(1432, $^3\Pi_{O^+g}$) → B(2431, $^3\Pi_{O^+g}$) transition, while the identity of the third band is ambiguous. Hemmati and Collins observed the D′(1432, $^3\Pi_{2g}$) → (2332, $^3\Delta_{2u}$) transition at 505 nm (19 802 cm^{-1}) with high buffer gas pressures. The observed band in this work peaks at 490 nm (20 408 cm^{-1}), a difference of 606 cm^{-1}, which is significant enough that it is most likely not the same transition. The higher energy of this band compared to that of the D′(1432, $^3\Pi_{2g}$) → (2332, $^3\Delta_{2u}$), coupled with its shape, hints that the transition may be from the E state to either a repulsive state or the continuum of a bound state. However, there is not enough evidence to make any kind of definitive assignment.

In their study of CH_2I_2, Dantus and co-workers found that molecular iodine was formed almost exclusively in the D′ state with little or no D or E state being observed.[3] In this work, the D′, D, and E states are significantly populated for CI_4, while for CHI_3, there is little population in the D′ and increased E state population. The presence of transitions from the E state can be explained by the slightly larger photolysis energy in this study (103 627 cm^{-1}) compared to that in the study by Dantus and co-workers (96 154 cm^{-1}). The difference of 7488 cm^{-1} is greater than the 5646 cm^{-1} energy difference between the E and D′ states. Also, while collisional electronic transfer from the D to E state is unlikely under experimental conditions, it cannot be completely ruled out.

The lack of a significant peak at 340 nm from the CHI_3 photodissociation, and its reappearance in CI_4, is somewhat puzzling. In their work on CH_2I_2, Dantus and co-workers use center of mass, as well as conservation of angular momentum, arguments to conclude that the CH_2 photofragment should contain a large amount of translational energy leading to an extremely large amount of orbital angular momentum excitation but little rotational energy. In this case, the orbital angular momentum is due to the relative motion of the two fragments as they fly apart.

The photodissociation of CHI_3 is different in three important ways. First, using a simple classical mechanical approach, we easily see that as the I_2 fragment detaches the recoil force will be directed on the central carbon of the carbene. For both CH_2 and CI_2, this means that the force will be directed at the center of mass, which would result in primarily translational motion. In HCI, however, the center of mass lies essentially at the position of the iodine atom. Therefore, applying a force to the carbon atom places a torque on the carbene resulting in rotational motion. Coupled with the fact that translational energy levels are basically continuous but rotational levels are quantitized, one would expect that HCI carries away less of the excess energy from the photodissociation. This in turn would increase the amount of energy, including electronic energy, available to the I_2 fragment. Because, as will be shown below, there is only 6000−20 000 cm^{-1} of excess energy after formation of excited-state HCI and I_2 and the D′ and E states of I_2 are so close energetically (∼800 cm^{-1}), it would only take a relatively small decrease in the energy of the carbene fragment to deplete the D′ and populate the E state of I_2.

The reappearance of the D′ → A′ transition in CI_4 is due to several factors. As mentioned above, the amount of rotational energy in the carbene fragment should be negligible; however, this is somewhat counterbalanced by the fact that the much larger reduced mass of CI_2 significantly lowers its vibrational frequencies relative to HCI. Therefore, it would be expected that the CI_2 photoproduct would have a much higher vibrational temperature than HCI, but this could not be confirmed experimentally. If the CI_2 fragment has a large amount of vibrational excitation, it would reduce the amount of energy available to the I_2 fragment for electronic excitation resulting in more I_2 in the D′ state. Because, as mentioned previously, collisions cannot be completely ruled out, some of the decrease in the D′ → A′ emission for CHI_3 compared to CI_4 could be due to the former being much less efficient at relaxing the singlet D state to the triplet D′.

A second difference between this work and that of Dantus and co-workers lies in the selection rules of the initial excitation. In this work, the excitation scheme involves a two-photon transition, while for that of Dantus, it is a three-photon excitation. Because a three-photon process has selection rules similar to that of a one-photon process and the total energies are different in both cases, it is safe to assume that different ion-pair states of the relevant photolytic precursors are being populated. To verify this, the photoproduct fluorescence from the photodissociation of CH_2I_2 was collected under our experimental conditions. This spectrum had large E → B and D → (2422, $^3\Sigma_{g(O^+)}$ or 2341, $^3\Sigma_{O^+g}$) transitions and a weak D′ → A′ transition. It should be noted that the D′ → A′ peak for CH_2I_2 was stronger than that from CHI_3 but weaker than that from CI_4.

The third and perhaps most important difference among CH_2I_2, CHI_3, and CI_4 is the energy difference between the singlet and triplet states of the carbene photofragments. Conservation of spin angular momentum requires that the sum of the orbital angular momenta of the photofragments equal that of the parent molecule. Because the parent molecule is a singlet, the fragments must both be either singlets or triplets. Recent high-level ab initio calculations have shown that for CH_2 the triplet ground state is 4436 cm^{-1} lower in energy than the first singlet state at the CASPT2/AE (6-311++G(3df,3pd)) level of theory.[21] Combined with the lower energy of Dantus's experiment, it is not surprising that only the triplet D′ I_2 is formed, but to be certain, detailed calculations on the reaction pathway would be necessary.

While the identity of the CI_2 ground state is still the subject of some debate, calculations at the same level of theory as those performed on CH_2 by Nguyen and co-workers indicate that the singlet−triplet gap is 2581 cm^{-1}. The exact energetics of CI_4 will be discussed in more detail in the following section; however, there is ample energy available to form both singlet and triplet CI_2 photoproduct. This explains the presence of transitions from the D, D′, and E states in Figure 2.

In HCI, the singlet−triplet gap was calculated to be only 339 cm^{-1}. This means that CHI_3 has 2258 cm^{-1} more energy, assuming all else is equal, available to the I_2 fragment when the excited-state carbene is formed than does CI_4. This is approximately 40% of the energy difference between the E and D′ states in I_2 and, coupled with the previous rotational and vibrational arguments, could explain the enhancement of the E and decrease in the D′ state of CHI_3 compared to CI_4.

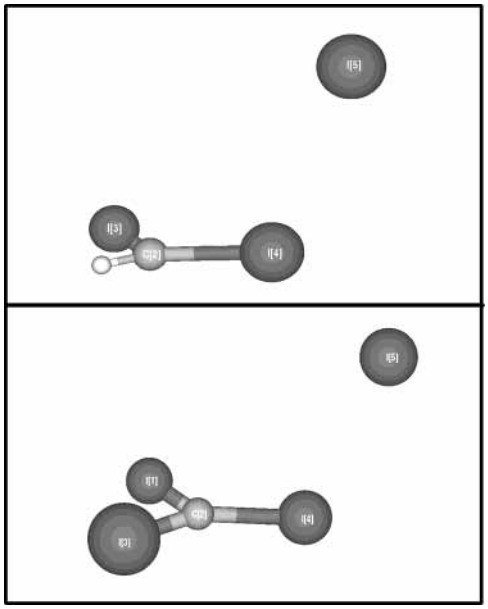

Figure 4. A schematic showing the atom numbering system used in the text for CHI_3 (upper panel) and CI_4 (lower panel). Both the CHI_3 and CI_4 structures shown are for the ion-pair isomer intermediates.

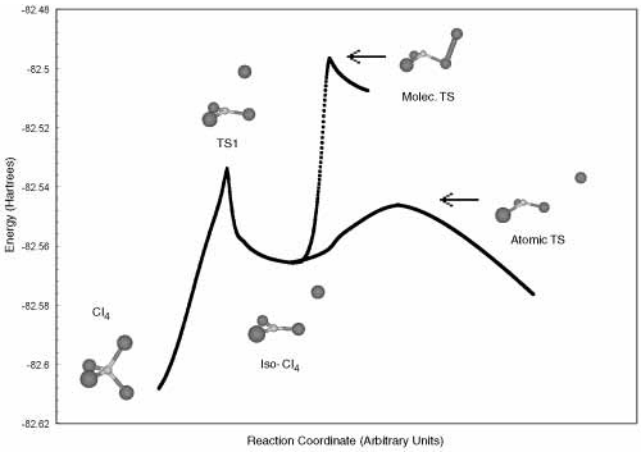

Figure 5. The calculated IRC for the ground-state dissociation of CI_4 along with selected structures. All energies and structures shown were calculated at the MP2 level of theory with the LANL2DZ basis.

C. Ab Initio Results. Even though the actual photodissociation takes place on an excited-state surface, the ground-state surface, that is, the formation of ground-state CI_2 ($^1A_1$) or HCI ($^1A'$) and I_2 ($^1\Sigma_g^+$) from ground-state CI_4 (CHI_3), is still illustrative of the overall mechanism. To better follow this mechanism, an atom numbering system has been adopted and is shown in Figure 4. In general, the mechanism and structures are similar for both the CI_4 and CHI_3 dissociations. Therefore, unless otherwise specified, CI_4 bond distances and angles will be used in the following discussion. Also, all of the energetic results reported in this section are based on the MP4 single-point calculations obtained using the MP2-optimized geometries.

The calculated IRCs at the MP2 level for ground-state CI_4 and CHI_3, along with stable structures and transition-state structures, are shown in Figures 5 and 6. Selected bond lengths, angles, and energies for these structures are given in Tables 1 and 2. For both molecules, there are three primary transition states, hereafter referred to as TS1, molec TS, and atomic TS, respectively. TS1 corresponds to a transition state from CI_4 or CHI_3 leading to formation of an ion-pair isomer of the parent molecule: either isoiodomethane, CI_3-I, or isoiodoform, CHI_2-

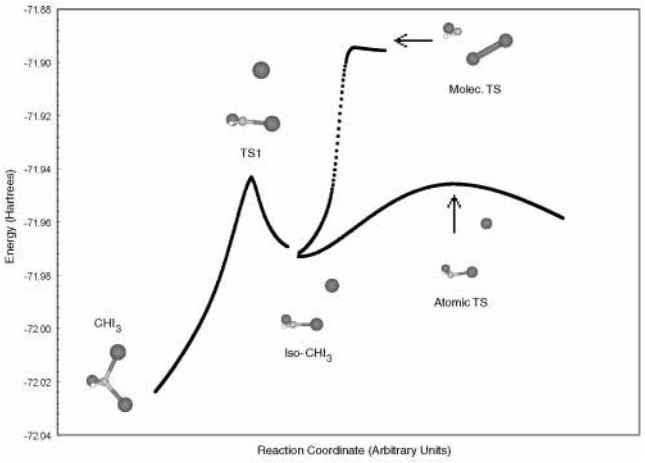

Figure 6. The calculated IRC for the ground-state dissociation of CHI_3 along with selected structures. All energies and structures shown were calculated at the MP2 level of theory with the LANL2DZ basis. The break in the IRC near the iso-CHI_3 structure is a computational artifact.

I. The reaction path to this transition state involves I5 migrating from its equilibrium position toward I4. In the reactant, the C2−I5 distance is 2.234 Å and the I4−I5 distance is 3.648 Å. At the TS1 structure, these distances have changed to 3.561 and 3.553 Å, respectively. This step is followed by the CI_3 moiety losing most of its pyramidal structure and becoming more planar. In CHI_3, the I3−C2−H1−I4 dihedral angle changes by 51.18° to 171.74° at the transition state. In CI_4, the change is less dramatic, but still significant, with the I1−C2−I3−I4 angle changing by 40.84°.

Even on the ground-state surface, significant charge transfer has already taken place when the system reaches TS1. The natural population analysis (NPA), summarized in Table 3, indicates that atom I5 has gained 0.406 electrons, which are redistributed from the other three iodine atoms. The two iodine atoms that will form the carbene donated the least density, just 0.075. Atom I4 loses the most electron density; its charge jumps from 0.277 to 0.530, a loss of 0.253 electrons. CHI_3 behaves in a similar manner with the exception that the charge differences are not as dramatic. This is not surprising because the hydrogen atom will be a poor donor of electron density compared to iodine. The energetic barrier to TS1, which is to formation of the ion-pair isomer, is 20 183 cm^{-1} for CHI_3 and 13 030 cm^{-1} for CI_4. In the actual experiment, the initial excitation contains 83 459 cm^{-1} of energy above TS1 for CHI_3 and 90 612 cm^{-1} for CI_4. This means that an ion-pair state is most likely formed first, and then the iodine migration occurs.

As the dissociation proceeds from TS1, the CI_3 moiety passes through the planer structure and I5 continues moving past I4 until it reaches one of the ion-pair isomer intermediates (iso-CHI_3 or iso-CI_4) shown in Figure 4. At this point, I5 has moved outside of I4 with the C2−I5 distance increasing to 4.490 Å and the I4−I5 distance decreasing to 3.296 Å. The CI_3 moiety has inverted with the I1−C2−I3−I4 dihedral angle changing by an additional 28.45° to −170.71°. CHI_3 also undergoes this inversion with a less dramatic change of angle. As would be expected, the charge separation is the largest for this structure. I5 now has a natural charge of −0.246, while I4 has increased to 0.599, a difference of 0.354 electrons. However, this does not lead to a fairly significant stabilization of iso-CI_4 with the well depth from TS1 being only 523 cm^{-1}. The same well is 7969 cm^{-1} for iso-CHI_3. This is not surprising because in iso-CHI_3 the charge separation is larger than that in iso-CI_4. The larger ionic charcter of iso-CHI_3 stabilizes it relative to iso-

TABLE 1: Selected Bond Distances (Å), Angles (deg), and Energies (au) for the Structures Shown in Figure 5[a]

parameter	CI_4	CI_4 TS1	iso-CI_4	CI_4 molec TS	CI_4 atomic TS	CI_2 product
r(I1−C2)	2.234	2.133	2.135	2.260	2.180	2.208
r(I3−C2)	2.234	2.133	2.135	2.260	2.180	2.208
r(I4−C2)	2.234	2.059	2.059	2.410	2.195	
r(I5−C2)	2.234	3.561	4.490	3.648	5.916	
r(I4−I5)	3.648	3.553	3.296	2.986	4.376	
∠I1−C2−I3	109.47	117.73	118.82	112.03	116.52	113.64
∠C2−I4−I5	35.28	73.37	111.89	84.36	125.02	
∠I1−C2−I3−I4	120.00	160.84	−170.71	124.96	136.61	
MP4 energy	−82.634 618	−82.575 247	−82.577 628	−82.506 436	−82.665 618	

[a] Geometrical parameters are from the structures optimized at the MP2 level of theory using the LANL2DZ basis set. MP4 single-point energies were obtained using geometries optimized at the MP2 level.

TABLE 2: Selected Bond Distances (Å), Angles (deg), and Energies (au) for the Structures Shown in Figure 6[a]

parameter	CHI_3	CHI_3 TS1	iso-CHI_3	CHI_3 molec TS	CHI_3 atomic TS	HCI product
r(H1−C2)	1.097	1.092	1.094	1.132	1.096	1.134
r(I3−C2)	2.205	2.091	2.108	2.232	2.138	2.163
r(I4−C2)	2.205	2.018	2.039	2.511	2.118	
r(I5−C2)	2.205	3.535	4.464	3.786	5.981	
r(I4−I5)	3.673	3.499	3.264	2.898	4.78	
∠H1−C2−I3	105.87	116.62	117.36	103.44	114.01	102.81
∠C2−I4−I5	33.56	74.30	112.61	88.56	114.65	
∠I3−C2−H1−I4	120.00	171.18	−171.74	113.98	−140.14	
MP4 energy	−72.057 803	−71.965 840	−72.000 215	−71.929 600	−72.053 130 9	

[a] Geometrical parameters are from the structures optimized at the MP2 level of theory using the LANL2DZ basis set. MP4 single-point energies were obtained using geometries optimized at the MP2 level.

TABLE 3: Natural Population Analysis of Selected Equilibrium Structures and Transition States on the CI_4 and CHI_3 Potential Energy Surfaces[a]

CHI_3		CI_4	
atom	natural charge	atom	natural charge
H(1)	0.246	C(2)	−1.107
C(2)	−0.946	I(1)	0.277
I(3)	0.233	I(3)	0.277
I(4)	0.233	I(4)	0.277
I(5)	0.233	I(5)	0.277
CHI_3 TS1		CI_4 TS1	
atom	natural charge	atom	natural charge
H(1)	0.242	C(2)	−1.104
C(2)	−0.928	I(1)	0.352
I(3)	0.349	I(3)	0.352
I(4)	0.560	I(4)	0.530
I(5)	−0.223	I(5)	−0.129
iso-CHI_3		iso-CI_4	
atom	natural charge	atom	natural charge
H(1)	0.232	C(2)	−1.011
C(2)	−0.842	I(1)	0.329
I(3)	0.292	I(3)	0.329
I(4)	0.575	I(4)	0.599
I(5)	−0.257	I(5)	−0.246
CHI_3 molec TS		CI_4 molec TS	
atom	natural charge	atom	natural charge
H(1)	0.147	C(2)	−0.791
C(2)	−0.627	I(1)	0.189
I(3)	0.115	I(3)	0.189
I(4)	0.315	I(4)	0.421
I(5)	0.051	I(5)	−0.008

[a] All calculations were obtained at the MP2 level of theory.

CI_4. This intermediate has been isolated experimentally for CH_2I_2 by Maier and Reisenauer[22] in a noble gas matrix; however, they did not report any bond lengths or angles that could be compared, even qualitatively, to our ab initio results. From the ion-pair states, two different pathways are possible. The first is elimination of an iodine atom to form CHI_2 + I or CI_3 + I through the atomic TS. The structures of the atomic transition states shown in Figures 5 and 6 are by no means the only ones possible. Several transition structures with nearly the same energy were found for both CHI_3 and CI_4. Those shown in the figures were randomly chosen. It should be noted that in the IRC calculations shown in Figures 3 and 4 the energy actually drops below that of the free radical products. This is a computational artifact due to the dissociation from a singlet transition state to doublet products. High-level configuration interaction calculations would avoid this problem; however, because this pathway is of little interest to the experiment, such calculations are beyond the scope of this work.

The second, more pertinent pathway is the formation of molecular products. From the ion-pair isomers, the reaction proceeds by elongation of the C2−I4 bond, while I5 moves back toward C2. The CI_3 moiety actually reinverts with I1−C2−I3−I4 dihedral angle changing by 64.33° to 124.96°. At the same time, the I4−I5 distance decreases to 2.986 Å. Although this is longer than the ground-state value of 2.666 Å, it is shorter than the D, D′, and E state equilibrium values, which are around 3.5 Å.[20] This indicates that the I_2 should have a large amount of vibrational excitation.

A key point is that in the structure of the molec TS the C_{2v} subsymmetry present in CI_4 has been broken, while for CHI_3, this subsymmetry does not exist to be broken. This result is in accord with Dantus' proposed asynchronous concerted dissociation mechanism, a key element of which involves symmetry breaking. This symmetry-broken structure was first proposed by Cain et al. on the basis of frontier Hückel molecular orbital calculations.[23] Their paper primarily focused on the addition reaction; however, their arguments are still valid for the dissociation. The Hückel calculations showed that the obvious insertion method, straightforward symmetric attack of the I_2 by the sp^2 electrons of the carbene, leads to a four-electron destabilization. This means that any insertion pathway that keeps the C_{2v} symmetry, for CX_2Y_2 molecules, is actually the highest

TABLE 4: Energy (cm^{-1}) of Several Possible Product Channels for the Photodissociation of CHI_3 and CI_4[a]

photoproducts	energy	excess energy[b]
HCI (singlet) + I_2 D(1441, $^1\Sigma_u^+$)	82 519	21 108
HCI (triplet) + I_2 D′(1432, $^3\Pi_2g$)	92 064	11 563
HCI (triplet) + I_2 E(1432, $^3\Pi_{O^+}g$)	97 710	5917
CI_2 (singlet) + I_2 D(1441, $^1\Sigma_u^+$)[c]	73 095	30 532
CI_2 (triplet) + I_2 D′(1432, $^3\Pi_2g$)	80 767	22 860
CI_2 (triplet) + I_2 E(1432, $^3\Pi_{Og}$)	86 413	17 214

[a] All reactant and product energies are from this work except the singlet−triplet gaps for HCI and CI_2, which are taken from ref 21. Excited-state I_2 energies were obtained by adding the vertical energy values of Mulliken[20] to the calculated ground-state values from this work. Energies are calculated relative to the CHI_3 (or CI_4) minimum. [b] Starting with 103 627 cm^{-1}. [c] Assuming singlet ground state.

in energy. The lower energy pathway is the nonsymmetric attack of the Lewis acidic p orbital on the central carbon of the carbene by a lone pair of the halogen. Their calculations predict an initial structure similar to the molec TS structure shown in Figures 5 and 6. This is not surprising because in the reverse (dissociation) mechanism one would expect the final structure to be similar to the initial structure of the addition reaction.

The NPA also confirms the work of Cain et al.[23] As the dissociation proceeds from the ion-pair isomer, both C2 and I5 lose charge. At the molec TS, C2 has lost 0.220 electrons and I5 has lost 0.239. Some of this loss is redistributed to I1 and I2 and the rest to I4. However, the key point is that I4 is still positively charged, while C2 and I5 are still negatively charged. This is not only in keeping with the work of Cain et al., but it shows that at the molec TS, which is a late transition state, there is still significant charge separation (0.429) between I4 and I5. This strongly suggests that I_2 is formed in an ion-pair state.

From the ion-pair isomer to the molec TS, there is an overall shift of 0.459 electrons, which means that this transition state would be expected to be high in energy. For CHI_3, the molec TS is 15 923 cm^{-1} above the ion-pair isomer and 28 137 cm^{-1} above initial reactant. For CI_4, it is 15 624 cm^{-1} above the ion-pair isomer and 28 133 cm^{-1} above the initial reactant. However, on the basis of the experimental excitation energy, in both cases, this leaves more than enough excess energy to form highly excited photoproducts. Table 4 shows the remaining energy for each product after 2×193 nm excitation. There is 5917−30 532 cm^{-1} of excess energy available to the photoproducts indicating that all photofragments should have significant translational, rotational (HCI only), and vibrational energy. It should also be noted that for CHI_3 forming the triplet HCI and I_2 in the E state requires 97 710 cm^{-1} of energy, which is 1556 cm^{-1} more energy than that available in Dantus' experiment. Because CH_2I_2 would be expected to have a larger barrier to molecular product formation than CHI_3, it is not surprising that they did not observe fluorescence from E state I_2.

V. Conclusions

The two-photon photodissociations of CI_4 and CHI_3 have been examined using both dispersed fluorescence and ab initio methods. With 103 627 cm^{-1} of available energy, the photoproduct fluorescence spectra from both molecules showed a mixture of I_2 in the D, D′, and E states. The D′ peak in the spectra arising from CHI_3 was found to be weaker than that from CI_4, while the E state emission band was enhanced.

The ab initio results show that the dissociation proceeds through a transition state to an ion-pair isomer. The isomer can then dissociate into an atomic or molecular product channel with the molecular channel having the largest barrier. The calculated IRC pathway and the structure of the molecular transition state agree well with the asynchronous concerted dissociation mechanism proposed by Dantus and co-workers.

Acknowledgment. We thank Dr. Jean Standard for help with the ab initio calculations and for a critical review of this paper prior to publication. Acknowledgment is made to the Illinois State University Research Grant program for support of portions of this work.

References and Notes

(1) Molina, M. J.; Moline, L. T.; Kolb, C. E. *Annu. Rev. Phys. Chem.* **1996**, *47*, 327.
(2) See, for example: Bergmann, K.; Carter, R. T.; Hall, G. E., Huber, J. R. *J. Chem. Phys.* **1998**, *109*, 474 and references therein.
(3) Marvet, U.; Zhang, Q.; Brown, E. J.; Dantus, M. *J. Chem. Phys.* **1998**, *109*, 4415.
(4) Zhang, Q.; Marvet, U.; Dantus, M. *J. Chem. Phys.* **1998**, *109*, 4428.
(5) Marvet, U.; Brown, E. J.; Dantus, M. *Phys. Chem. Chem. Phys.* **2000**, *2*, 885.
(6) Farmanara, P.; Stert, V.; Ritze, H.-H.; Radloff, W. *J. Chem. Phys.* **2000**, *111*, 1705.
(7) Frisch, M. J.; Trucks, G. W.; Schlegel, H. B.; Scuseria, G. E.; Robb, M. A.; Cheeseman, J. R.; Zakrzewski, V. G.; Montgomery, J. A., Jr.; Stratmann, R. E.; Burant, J. C.; Dapprich, S.; Millam, J. M.; Daniels, A. D.; Kudin, K. N.; Strain, M. C.; Farkas, O.; Tomasi, J.; Barone, V.; Cossi, M.; Cammi, R.; Mennucci, B.; Pomelli, C.; Adamo, C.; Clifford, S.; Ochterski, J.; Petersson, G. A.; Ayala, P. Y.; Cui, Q.; Morokuma, K.; Malick, D. K.; Rabuck, A. D.; Raghavachari, K.; Foresman, J. B.; Cioslowski, J.; Ortiz, J. V.; Stefanov, B. B.; Liu, G.; Liashenko, A.; Piskorz, P.; Komaromi, I.; Gomperts, R.; Martin, R. L.; Fox, D. J.; Keith, T.; Al-Laham, M. A.; Peng, C. Y.; Nanayakkara, A.; Gonzalez, C.; Challacombe, M.; Gill, P. M. W.; Johnson, B. G.; Chen, W.; Wong, M. W.; Andres, J. L.; Head-Gordon, M.; Replogle, E. S.; Pople, J. A. *Gaussian 98*, revision A.7; Gaussian, Inc.: Pittsburgh, PA, 1998.
(8) Hay P. J.; Wadt, W. R. *J. Chem. Phys.* **1985**, *82*, 270.
(9) Hay P. J.; Wadt, W. R. *J. Chem. Phys.* **1985**, *82*, 284.
(10) Hay P. J.; Wadt, W. R. *J. Chem. Phys.* **1985**, *82*, 299.
(11) Dunning, T. H., Jr.; Hay, P. J. In *Modern Theoretical Chemistry*; Schaefer, H. F., III, Ed.; Plenum: New York, 1976; pp 1−28.
(12) Glendening, E. D.; Badenhoop, J. K.; Reed, A. E.; Carpenter, J. E.; Weinhold, F. *NBO 4.0*; Theoretical Chemistry Institute, University of Wisconsin: Madison, WI, 1996.
(13) Reed, A. E.; Weinhold, F. *J. Chem. Phys.* **1983**, *78*, 4066.
(14) Reed, A. E.; Weinstock, R. B.; Weinhold, F. *J. Chem. Phys.* **1985**, *83*, 735.
(15) Kawasaki, M.; Lee, S. J.; Bersohn, R. *J. Chem. Phys.* **1975**, *63*, 809.
(16) Okabe, H.; Kawasaki, M.; Tanake, Y. *J. Chem. Phys.* **1980**, *73*, 6162.
(17) Dyne, P. J.; Style, D. W. G. *J. Chem. Soc.* **1952**, 2122.
(18) Style, D. W. G.; Ward, J. C. *J. Chem. Soc.* **1952**, 2125.
(19) Hemmati, H.; Collins, G. J. *Chem. Phys. Lett.* **1980**, *75* (3), 488.
(20) Mulliken, R. S. *J. Chem. Phys.* **1971**, *55*, 288.
(21) Hajgato, B.; Nguyen, H. M. T.; Veszprémi, T.; Nguyen, M. T. *Phys. Chem. Chem. Phys.* **2000**, *2*, 5041.
(22) Maier, G.; Reisenauer, H. P. *Angew. Chem., Int. Ed. Engl.* **1986**, *25*, 819.
(23) Cain, S. R.; Hoffmann, R.; Grant, E. R. *J. Phys. Chem.* **1981**, *85*, 4046.